

# Carbon-hydrogen defects with a neighboring oxygen atom in n-type Si

K. Gwozdz,<sup>1</sup> R. Stübner,<sup>2</sup> V. Kolkovsky,<sup>2,a)</sup> and J. Weber<sup>2</sup>

<sup>1</sup>Department of Quantum Technologies, Faculty of Fundamental Problems of Technology, Wrocław University of Science and Technology, Wybrzeże Wyspiańskiego 27, 50-370 Wrocław, Poland

<sup>2</sup>Technische Universität Dresden, 01062 Dresden, Germany

(Received 22 February 2017; accepted 28 June 2017; published online 17 July 2017)

We report on the electrical activation of neutral carbon-oxygen complexes in Si by wet-chemical etching at room temperature. Two deep levels, E65 and E75, are observed by deep level transient spectroscopy in *n*-type Czochralski Si. The activation enthalpies of E65 and E75 are obtained as  $E_C - 0.11$  eV (E65) and  $E_C - 0.13$  eV (E75). The electric field dependence of their emission rates relates both levels to single acceptor states. From the analysis of the depth profiles, we conclude that the levels belong to two different defects, which contain only one hydrogen atom. A configuration is proposed, where the  $\text{CH}_{1\text{BC}}$  defect, with hydrogen in the bond-centered position between neighboring C and Si atoms, is disturbed by interstitial oxygen in the second nearest neighbor position to substitutional carbon. The significant reduction of the  $\text{CH}_{1\text{BC}}$  concentration in samples with high oxygen concentrations limits the use of this defect for the determination of low concentrations of substitutional carbon in Si samples. *Published by AIP Publishing.*

<http://dx.doi.org/10.1063/1.4993934>

The mutation of neutral contaminants into electrically active defects during processing of electronic devices is detrimental to their performance.<sup>1,2</sup> In silicon grown by the Czochralski (CZ) method, the dominant electrical neutral contaminations are oxygen on interstitial and carbon on substitutional lattice sites. However, C can be electrically activated, e.g., by the interaction with Si self-interstitials generated during ion-implantation or oxygen-precipitation. Treatments of the samples in a H-plasma, H implantation, or wet chemical etching (WCE) lead to another, unexpected activation mechanism of the neutral carbon by atomic hydrogen.<sup>3–10</sup> The negative influence of the electrically active carbon defects on device performance in modern advanced power devices, photodetectors, and high efficiency solar cells asks today for carbon concentrations below  $10^{13}$ – $10^{14}$  cm<sup>−3</sup>.<sup>11,12</sup> However, the conventional detection limit for substitutional C by Fourier transform infrared (FTIR) absorption is only around  $2 \times 10^{15}$  cm<sup>−3</sup>.<sup>13</sup> Therefore, an improvement of the FTIR absorption or alternative techniques are needed to detect lower C-concentrations.<sup>11,12,14,15</sup>

Recently, Samata *et al.* suggested a new approach for detecting low C concentrations in *n*-type Si with the help of deep level transient spectroscopy (DLTS).<sup>11</sup> The DLTS technique allows the detection of electrically active defects with concentrations as small as  $10^{10}$ – $10^{11}$  cm<sup>−3</sup> in samples with shallow doping levels of around  $10^{14}$ – $10^{15}$  cm<sup>−3</sup>. The new proposal in Ref. 11 uses the concentration of one of the electrically active CH-related defects, labeled E3, as a probe for the total C concentration in silicon wafers. The method could be successful if the concentration of the CH-related defect is not influenced by the presence of other impurities such as oxygen in the samples. The brevity of Ref. 11 does not allow an identification of the used CH-defect with known defects from the literature [e.g.,  $\text{CH}_{1\text{BC}}$  or  $\text{CH}_\text{B}$  (Ref. 6)].

In the present work, we report on the strong reduction of a CH-related DLTS level (labeled  $\text{CH}_{1\text{BC}}$  in Ref. 6 and E90 in the following) in samples with an interstitial oxygen ( $\text{O}_\text{i}$ ) concentration above  $10^{17}$  cm<sup>−3</sup>. Two different defects (E65 and E75) appear in the DLTS spectra of these samples and they have been previously assigned either to defects induced by resistive evaporation of metal Schottky contacts<sup>10</sup> or to defects introduced by wet chemical etching.<sup>7</sup> Yoneta *et al.*<sup>7</sup> reported on an increase in these defects with the concentration of oxygen and carbon in Si and assigned them to two COH-related complexes. At present, the origin and charge states of the defects are controversial. We will show that the levels E65 and E75 belong to two different single acceptors, which have electrical properties such as the E90 defect, which was identified as the bond centered hydrogen atom next to carbon ( $\text{CH}_{1\text{BC}}$ ).<sup>6</sup>

Samples were cut from one Float Zone (FZ) (sample #1) and four different electronic grade CZ Si wafers (samples #2 to #5) with different concentrations of carbon and oxygen. Table I summarizes the concentrations of phosphorus, carbon, and oxygen in these samples. Hydrogen was introduced by wet chemical etching (WCE) at room temperature (RT) for 2 minutes in an acid consisting of  $\text{HNO}_3$ : $\text{HF}$ : $\text{CH}_3\text{COOH}$  with a volume ratio of 5:3:3. Schottky diodes were produced

TABLE I. List of samples investigated in the present study. The concentrations are given by the vendors and were determined by resistivity measurements (P) and FTIR absorption ( $\text{O}_\text{i}$ ,  $\text{C}_\text{s}$ ) using the appropriate SEMI standards.

Name	[P] (cm <sup>−3</sup> )	[C <sub>s</sub> ] (cm <sup>−3</sup> )	[O <sub>i</sub> ] (cm <sup>−3</sup> )
Sample #1	$2 \times 10^{15}$	$< 5 \times 10^{15}$	$5 \times 10^{15}$
Sample #2	$2 \times 10^{15}$	$< 5 \times 10^{15}$	$1 \times 10^{18}$
Sample #3	$1 \times 10^{15}$	$2 \times 10^{16}$	$1 \times 10^{18}$
Sample #4	$2 \times 10^{14}$	$4.5 \times 10^{14}$	$5 \times 10^{17}$
Sample #5	$2 \times 10^{14}$	$9 \times 10^{14}$	$5 \times 10^{17}$

<sup>a)</sup> Author to whom correspondence should be addressed: kolkov@ifpan.edu.pl

by resistive evaporation of Au in vacuum onto the polished side of the samples at room temperature. Rubbing the back side of the samples with a eutectic InGa alloy generated Ohmic contacts. The Schottky and Ohmic contacts were characterized by current-voltage ( $I$ - $V$ ) and capacitance-voltage ( $C$ - $V$ ) measurements in the range of 50–300 K. The thermal stability of the defects was investigated by 30 min isochronal anneals in air in the range of 310–410 K.  $C$ - $V$  measurements were performed at 1 MHz with a Boonton 7200 capacitance meter. Laplace DLTS<sup>16</sup> with two filling pulses was employed to investigate the electronic properties (activation enthalpy and capture cross section) of deep levels and their depth profiles. The labeling of the DLTS peaks in this work corresponds to the temperatures at which the peaks were observed in the DLTS spectra for an emission rate of  $48 \text{ s}^{-1}$ . Deep level concentration profiles were measured by Laplace DLTS at a fixed reverse bias while varying the two pulse biases. From the  $C$ - $V$  profile, the electrical field was calculated as described in Ref. 17. The influence on the emission rate by the electric field was studied at fixed pulse biases while varying the reverse bias.

Figure 1 shows DLTS spectra from samples #1 to #5 after hydrogen introduction by WCE. In the sample with the lowest oxygen concentration (sample #1), E90 was detected at about 90 K. The electrical properties of this level are identical to those reported from the  $\text{CH}_{1\text{BC}}$  center.<sup>6</sup> In the samples with higher oxygen concentrations (samples #2 to #5), the concentration of E90 was below the detection limit of our DLTS setup ( $\approx 10^{11} \text{ cm}^{-3}$  for the samples #2 and #3 and  $\approx 5 \times 10^{10} \text{ cm}^{-3}$  for the samples #4 and #5). Instead, two other dominant peaks E65 and E75 show up at lower temperatures of 65 K and 75 K, respectively. In samples #2, #4, and #5, additional DLTS peaks E55 and E60 appear. These peaks are related to residual thermal donors, and their intensities and positions change after annealing of the samples at temperatures around 450 °C. In our present study, we will focus only on the discussion of the origin of E65 and E75.

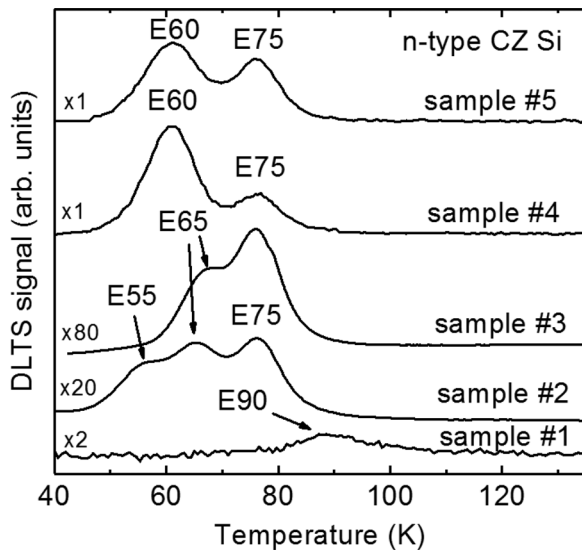


FIG. 1. DLTS spectra from different  $n$ -type Si samples after wet chemical etching. DLTS signals are reduced for different spectra for a better comparison according to the given factors. All spectra are recorded with a rate window of  $48 \text{ s}^{-1}$ .

Laplace DLTS spectra from all samples were recorded. Due to the increased resolution, E75 and E65 could be resolved in samples #2 to #5; however, the intensity of E65 was weak in samples #4 and #5. Figure 2 presents Laplace DLTS spectra from sample #2 after WCE (sample temperature, 77 K). The two peaks corresponding to E65 and E75 were resolved. Level E55 has an emission rate of more than  $10^4 \text{ s}^{-1}$  at this temperature and escapes detection in Fig. 2. The Arrhenius plots (inset of Fig. 2) yield the activation enthalpies of the defects as  $E_C - 0.11 \text{ eV}$  (E65) and  $E_C - 0.13 \text{ eV}$  (E75) and the apparent capture cross sections of  $2 \times 10^{-16} \text{ cm}^2$  (E65) and  $9 \times 10^{-16} \text{ cm}^2$  (E75). The capture cross section was also directly determined from measurements of the intensity of E65 and E75 as a function of the filling pulse width. These values are about  $2 \times 10^{-18} \text{ cm}^2$  for E65 and E75, respectively. We did not observe any temperature dependence of the capture cross sections. This indicates the absence of a capture barrier for electrons and allows us to calculate the entropy changes for E65 and E75 as  $4.6k$  (E65) and  $6.1k$  (E75) during emission of the carriers.

Laplace DLTS spectra with reverse biases varying in the range between  $-2 \text{ V}$  and  $-7 \text{ V}$  were recorded for E65 and E75 in sample #2. The emission rates of the levels as a function of the electric field are presented in Fig. 3. Both levels show an enhancement of the emission rate as a function of the electric field. However, this enhancement is significantly smaller than that expected for donor states, which obey the three-dimensional Poole-Frenkel model<sup>18</sup> (dashed line in Fig. 3). A square-well potential characteristic for defects, which are neutral after emission of an electron in  $n$ -type Si, satisfactorily describes our experimental data (solid line in Fig. 3). The field dependence of the emission rate varies according to<sup>18</sup>

$$e = e_0 \left[ (2\gamma E)^{-1} (\exp(\gamma E) - 1) + 0.5 \right],$$

where  $\gamma = qr/kT$  with the elementary charge  $q$ , Boltzmann constant  $k$ , temperature  $T$ , and the radius of the square-well potential  $r$ . A best fit of the experimental data given in Fig. 3

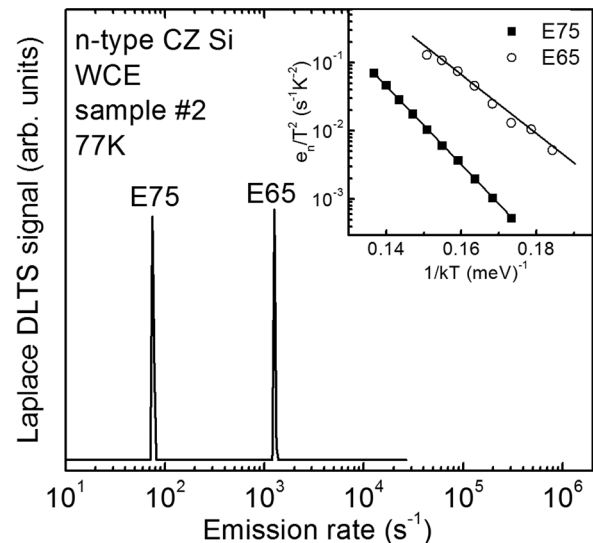


FIG. 2. Laplace DLTS spectrum from sample #2 after wet chemical etching. The inset shows Arrhenius plots of peaks E65 and E75.

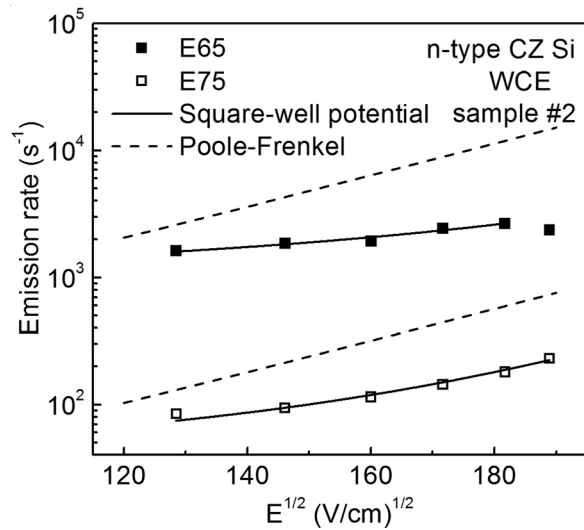


FIG. 3. Emission rate of E65 and E75 as a function of the square-root of the electric field. The dependence from the three-dimensional Poole-Frenkel model of a Coulombic center is shown as the dashed line. The fit of the experimental data within the model of neutral defects (square-well potential) is given as the solid line.

was achieved for a square-well potential with radii of 4.5 nm (E65) and 6.5 nm (E75), respectively.

Concentration depth profiles of E65 and E75 in sample #3 are presented in Fig. 4(a). The profiles were recorded directly after WCE at RT by Laplace DLTS. During WCE, donor passivation occurs by bonding of one hydrogen atom to the phosphorus donor.<sup>19</sup> The profile of the phosphorous-hydrogen (PH) complex in this figure was obtained by subtraction of the net free carrier concentration in the hydrogenated sample from that before hydrogenation. The concentration of all levels decreases with depth, and the slope is identical for PH, E65, and E75. The depth profiles in sample #2 (not shown) show the same slope for E65 and E75 but with smaller total concentrations, due to the lower  $C_S$  concentration.

In Fig. 4(b), the depth profiles of E75 and PH are given for samples #4 and #5. Their concentration also decreases towards the bulk of Si, and the slope of the reduction is identical. Due to the lower signal to noise ratio, the depth profiles of E65 could not be properly determined in these samples. The depth profile of the thermal donors (E60) shows a reduced concentration close to the sample surface due to hydrogen passivation and a constant concentration in the bulk.

Figure 5 presents the thermal stability of E65 and E75 in sample #3 after 30 min isochronal annealing steps in the range of 310–410 K. The concentration of both defects is approximately constant up to 340 K and vanishes at about 380 K. No traces of the defects or new defect levels were detected after the anneal above 410 K.

Our results confirm the work by Yoneta *et al.*<sup>7</sup> that E65 and E75 contain oxygen, carbon, and hydrogen. These levels are not observed in samples with low oxygen concentrations (sample #1), whereas the concentration of these defects increases significantly in samples with a higher oxygen content (samples #2 to #3). In addition, we verified that the concentration of the defects was increased in samples with a higher H content, which could be generated by a dc H

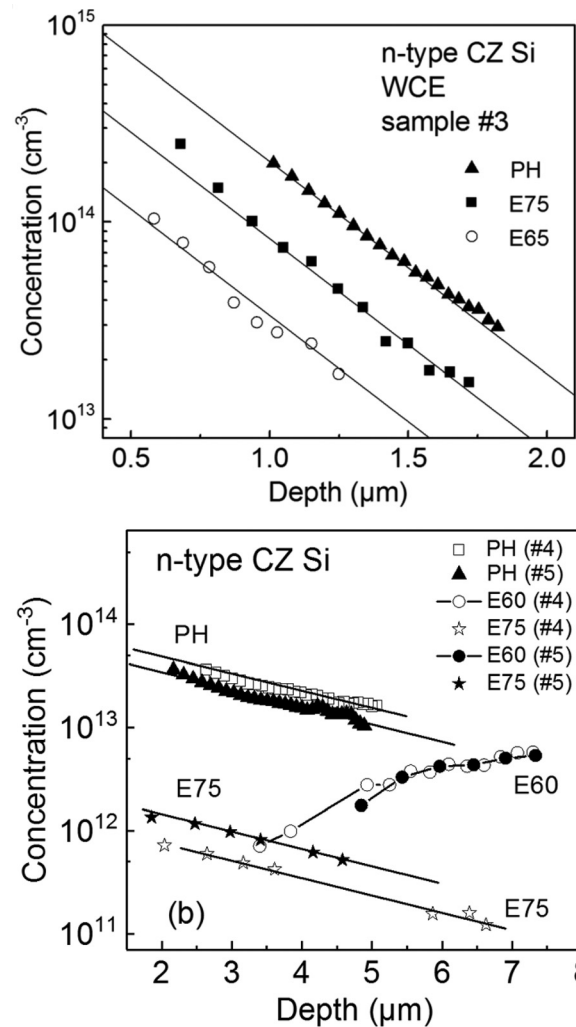


FIG. 4. Depth profiles determined from Laplace DLTS measurements and C-V profiling of E65, E75, and PH complexes for sample #3 (a) and for E75 and PH complexes for samples #4 and #5 (b).

plasma treatment, WCE with higher etch rates, or prolonged WCE.

The concentration of hydrogen-related defects introduced by WCE was shown to decrease towards the bulk

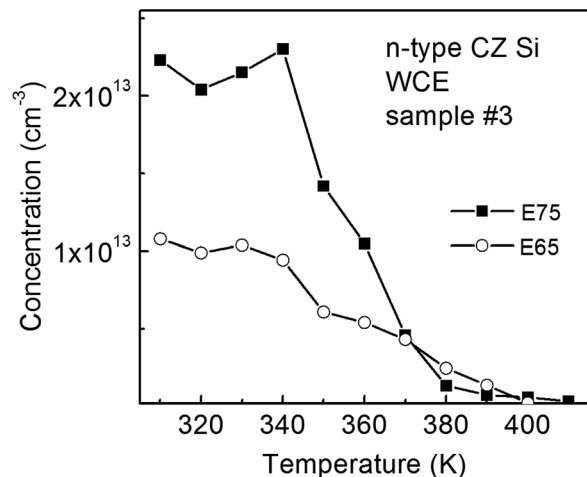


FIG. 5. The concentration determined at a depth of  $\sim 1.5 \mu\text{m}$  of E65 and E75 versus annealing temperature measured after isochronal annealing steps of 30 min.



with a slope that was proportional to  $\exp(-ix/L)$ , where  $i$  was the number of hydrogen atoms in the complex and  $L$  the characteristic penetration depth of the hydrogen species.<sup>20</sup> Therefore, the number of hydrogen atoms in these complexes can be directly derived if one compares the concentration of different hydrogen-related defects as a function of depth. The concentration profiles of E65 and E75 are identical to the profile of the passivated phosphorus donor (PH) (Fig. 4), which demonstrate that the defects also contain only one H atom.

The electrical fingerprints of E65 and E75 such as activation enthalpy, capture cross section, and the dependence of the emission rate on the electric field are similar, and both levels anneal out almost simultaneously at about 380 K. Both E65 and E75 are single acceptors since the enhancement of their emission rate is lower compared to the three-dimensional Poole-Frenkel model, which is characteristic of a defect with a Coulombic potential. We describe the single acceptor in  $n$ -type Si as a neutral center which binds the electron in a square well potential.<sup>18</sup> Our values for the radius of the potential resemble those of other single acceptors from the literature.<sup>6,21,22</sup> The small capture cross sections of E65 and E75 (around  $2 \times 10^{-18} \text{ cm}^2$ ) is also consistent with the acceptor-like behavior of these centers.

The electrical properties of E65 and E75 and their annealing behavior are very similar to those of the  $\text{CH}_{\text{IBC}}$  complex (E90).<sup>3–6</sup> It is suggestive to attribute E65 and E75 to the  $\text{CH}_{\text{IBC}}$  complex disturbed by the presence of an oxygen atom in its nearest neighborhood. E65 and E75 do not belong to different charge states of the same defect due to the same dependence of their emission rate on the electric field, and they do not belong to the same defect since their depth profiles are different. Therefore, the appearance of two DLTS peaks E65 and E75 could be explained by non-equivalent orientations of  $\text{O}_i$  with respect to  $\text{CH}_{\text{IBC}}$ . Newman and Willis first identified pairs of substitutional carbon with interstitial oxygen ( $\text{C}_s\text{O}_i$ ) in as grown CZ-Si samples by infrared absorption.<sup>23</sup> The most stable pair has  $\text{C}_s$  at the second neighbor site of  $\text{O}_i$ .<sup>24,25</sup> The hydrogen interaction with the  $\text{C}_s\text{O}_i$  complex could lead to two different structures  $\text{C-H}_{\text{BC}}\text{-Si-O}_i$  or  $\text{H}_{\text{BC}}\text{-C-Si-O}_i$ . For the first one, a strong shift of the  $\text{CH}_{\text{IBC}}$  electronic level is expected. In the second configuration,  $\text{H}_{\text{BC}}$  would only be slightly disturbed by the oxygen atom in the next-nearest neighbor position and only slight shifts of the electronic levels would be expected. The two levels E65 and E75 could be indicative of the two inequivalent positions of H in this second configuration. However, calculations are necessary to understand the exact structure of these complexes.

The absence of the  $\text{CH}_{\text{IBC}}$  complex in samples with a high concentration of oxygen agrees with a preferential formation of  $\text{C}_s\text{O}_i$  pairs indicated in Ref. 22 and/or a more efficient trapping of H at these defects. The determination of  $\text{C}_s$  from only the  $\text{CH}_{\text{IBC}}$  concentration, as proposed by Samata *et al.*,<sup>11</sup> is therefore questionable. Even in samples with an identical oxygen concentration, the depth profiles of the defects and their dependence on WCE conditions will prevent a direct comparison of the CH concentrations.

To summarize, two different defects E65 and E75 were detected in Si samples with high oxygen concentrations ( $>10^{17} \text{ cm}^{-3}$ ). The analysis of the electrical properties of these defects showed that both were single acceptors with capture cross sections of about  $2 \times 10^{-18} \text{ cm}^2$ . The depth profiles of E65 and E75 demonstrated that these defects contain one hydrogen atom. We attribute them to the  $\text{CH}_{\text{IBC}}$  configuration of the CH complex with an additional oxygen atom in its next-nearest neighborhood. Based on our results, the proposed method in Ref. 11 of low carbon concentration detection in silicon is not valid in samples with larger oxygen concentrations.

The samples in this study were generously supplied by Siltronic AG and GlobalWafers Japan Co., Ltd. K. Gwozdz would like to thank the Faculty of Fundamental Problems of Technology of the Wroclaw University for financial support from the special-purpose grant awarded by the Ministry of Science and Higher Education in 2016 for research and development of young scientists and PhD students and DAAD for the support of her stay in Dresden. L. Scheffler performed first preliminary measurements on these samples.

<sup>1</sup>W. Bullis, *Mater. Sci. Eng.*, **B 72**, 93 (2000).

<sup>2</sup>H. J. Queisser and E. E. Haller, *Science* **281**, 945 (1998).

<sup>3</sup>A. Endrös, *Phys. Rev. Lett.* **63**, 70 (1989).

<sup>4</sup>Y. Kamiura, M. Tsutsue, Y. Tamashita, F. Hashimoto, and K. Okuno, *J. Appl. Phys.* **78**, 4478 (1995).

<sup>5</sup>O. Andersen, A. R. Peaker, L. Dobaczewski, K. B. Nielsen, B. Hourahine, R. Jones, P. R. Briddon, and S. Öberg, *Phys. Rev. B* **66**, 235205 (2002).

<sup>6</sup>R. Stübner, V. I. Kolkovsky, and J. Weber, *J. Appl. Phys.* **118**, 055704 (2015).

<sup>7</sup>M. Yoneta, Y. Kamiura, and F. Hashimoto, *J. Appl. Phys.* **70**, 1295 (1991).

<sup>8</sup>R. Stübner, L. Scheffler, V. I. Kolkovsky, and J. Weber, *J. Appl. Phys.* **119**, 205709 (2016).

<sup>9</sup>Y. L. Huang, E. Simoen, C. Claeys, J. M. Rafi, and P. Clauws, *J. Mater. Sci. Mater. Electron.* **18**, 705 (2007).

<sup>10</sup>F. D. Aurret, R. Kleinhenz, and C. P. Schneider, *Appl. Phys. Lett.* **44**, 209 (1984).

<sup>11</sup>S. Samata, K. Eriguchi, and N. Mitsugi, in *5th Seminar of Advanced Power Semiconductors*, Japan Society of Applied Physics (2016), Vol. 3, p. 1.

<sup>12</sup>H. Furuya, in *The 7-th International Symposium on Advanced Science and Technology of Silicon Materials* (2016), Vol. 1–6, p. 21.

<sup>13</sup>SEMI MF-1391-1107, 2004.

<sup>14</sup>H. C. Alt, Y. Gomeniuk, B. Wiedemann, and H. Riemann, *J. Electrochem. Soc.* **150**, G498 (2003).

<sup>15</sup>N. Inoue, *Phys. Status Solidi C* **13**, 842 (2016).

<sup>16</sup>L. Dobaczewski, A. R. Peaker, and K. B. Nielsen, *J. Appl. Phys.* **96**, 4689 (2004).

<sup>17</sup>P. Blood and P. W. Orton, *The Electrical Characterization of Semiconductors: Majority Carriers and Electron States* (Academic Press, 1992).

<sup>18</sup>J. L. Hartke, *J. Appl. Phys.* **39**, 4871 (1968).

<sup>19</sup>K. Bergman, M. Stavola, S. J. Pearton, and J. Lopata, *Phys. Rev. B* **37**, 2770 (1988).

<sup>20</sup>O. V. Feklisova, E. B. Yakimov, and N. A. Yarykin, *Semiconductors* **36**, 282 (2002).

<sup>21</sup>N. Baber, H. Scheffler, A. Ostmann, T. Wolf, and D. Bimberg, *Phys. Rev. B* **45**, 4043 (1992).

<sup>22</sup>Q. S. Zhu, K. Hiramatsu, N. Sawaki, I. Akasaki, and X. N. Liu, *J. Appl. Phys.* **73**, 771 (1993).

<sup>23</sup>R. C. Newman and J. B. Willis, *J. Phys. Chem. Solids* **26**, 373 (1965).

<sup>24</sup>G. Davies and R. V. Newman, *Handbook on Semiconductors* (Elsevier, Amsterdam, 1994), Vol. 3.

<sup>25</sup>Y. Shirakawa and H. Y. Kaneta, *J. Appl. Phys.* **80**, 4199 (1996).